Journal of Inorganic Biochemistry 219 (2021) 111385

Contents lists available at ScienceDirect

Journal of Inorganic Biochemistry

journal homepage: www.elsevier.com/locate/jinorgbio

Development of new combination anti-leishmanial complexes: Triphenyl Sb (V) *mono*-hydroxy *mono*-quinolinolates

Rebekah N. Duffin [a], Victoria L. Blair [b], Lukasz Kedzierski [c], Philip C. Andrews [b,*]

[a] Faculty of Pharmacy and Pharmaceutical Sciences, Drug delivery, disposition and dynamics, Monash University, Parkville, Melbourne, VIC 3053, Australia
[b] School of Chemistry, Monash University, Clayton, Melbourne, VIC 3800, Australia
[c] Faculty of Veterinary and Agricultural Sciences, The Peter Doherty Institute for Infection and Immunity, 792 Elizabeth Street, Melbourne 3000, Victoria, Australia

ARTICLE INFO

Keywords:
Leishmania
Antimony
Organometallic
Hydroxyquinolines
Combination drugs

ABSTRACT

In seeking to develop single entity combination anti-Leishmanial complexes six heteropletic organometallic Sb (V) hydroxido quinolinolate complexes of general formula $[SbPh_3(C_9H_4NORR')(OH)]$ have been synthesised and characterised, derived from a series of halide substituted quinolinols (8-hydroxyquinolines). Single crystal X-ray diffraction on all the complexes show a common distorted six-coordinate octahedral environment at the Sb(V) centre, with the aryl groups and nitrogen atom of quinolinolate ligand bonding in the equatorial planes, with the two oxygen atoms (hydroxyl and quinolinolate) occupying the axial plane in an almost linear configuration. Each complex was tested for their anti-promastigote activity and mammalian cytotoxicity and a selectivity indices established. The complexes displayed excellent anti-promastigote activity (IC_{50}: 2.03–3.39 μM) and varied mammalian cytotoxicity (IC_{50}: 12.7–46.9 μM), leading to a selectivity index range of 4.52–16.7. All complexes displayed excellent anti-amastigote activity with a percentage infection range of 2.25%–9.00%. All complexes performed substantially better than the parent quinolinols and comparable carboxylate complexes $[SbPh_3(O_2CRR')_2]$ indicating the synergistic role of the Sb(V) and quinolinol moieties in increasing parasite mortality. Two of the complexes $[SbPh_3(C_9H_4NOBr_2)(OH)]$ 4, $[SbPh_3(C_9H_4NOI_2)(OH)]$ 5, provide an ideal combination of high selective and good activity towards the leishmanial amastigotes and offer the potential as good lead compounds.

1. Introduction

The prevalence of neglected tropical disease (NTDs) worldwide are advancing at an alarming rate. Leishmaniasis falls within this category, localised in over 100 countries with 550 million people at risk of infection [1,2]. A proportion of these incidences (~400,000) result in the deadliest form of the disease, visceral leishmaniasis (VL), of which approximately 10% of cases result in death [3,4]. Without immediate treatment, VL is often lethal [3,5]. The first-line treatment for VL involves the use of intravenous pentavalent antimonials; Pentostam™ (sodium stibogluconate, SSG) and Glucantime™ (meglumine antimoniate), these drugs are effective but harbour problems with toxicity and unavoidable side-effects [6]. In serious cases the use of these antimonials can lead to cardiotoxicity and pancreatitis [7]. Increased resistance is also undermining their efficacy [8]. Other treatments such as orally available miltefosine, amphotericin B and pentamidine harbour problems with teratogenicity, expense and toxicity respectively (Fig. 1) [9–12].

The mechanism by which the Sb(V) drugs interact with the parasite is not fully understood, however there are several evidence-supported hypotheses. The most commonly accepted theory is based on reductive bio-conversion of the Sb(V) to Sb(III) by either the host cell or the parasite itself [13]. This Sb(V) to Sb(III) reduction is more efficient in a low pH environment such as the intracellular amastigote [14]. Sb(III) then forms a conjugate pair with the parasitic thiol trypanothione, an important virulence factor of *Leishmania*, causing inactivation of its biological process [15]. An alternative mechanism proposed suggests the Sb(V) acts directly on the parasite. It is theorised the Sb(V) exerts activity by acting on protein phosphokinases causing a cascade effect leading to eventual cell death, therefore the use of Sb(V) as the central moiety in these potential combination drugs may exert a more synergistic effect than first predicted [14].

Two of the most significant challenges in developing new anti-Leishmanial drugs is in offsetting inherent toxicity and resistance

* Corresponding author.
E-mail address: phil.andrews@monash.edu (P.C. Andrews).

https://doi.org/10.1016/j.jinorgbio.2021.111385
Received 5 November 2020; Received in revised form 20 January 2021; Accepted 27 January 2021
Available online 10 February 2021
0162-0134/© 2021 Elsevier Inc. All rights reserved.

[12,16–18]. One key approach is in using combination therapy with known antimicrobial drug combinations [6,19–23]. This has shown some success in improving compliance and treatment times, reducing the overall drug-load, reducing overall toxic effects on the body, and providing more cost-effective treatment regimens. Where monotherapy with SSG or Glucantime has become, or is becoming ineffective, such as areas of India, Africa, the Mediterranean and South America, then combination therapies with paromomycin and/or liposomal amphotericin B (LAmB) are already recommended as the primary treatment regimen [24].

Our focus has been on designing and developing complexes which offer the potential for different solubility, activity, toxicity, and mode(s)-of-action, and have thus far focussed on organometallic Sb(V) complexes as more lipophilic chemical entities compared with traditional Sb(V) drugs. We have shown that the class of *tris*-aryl *bis*-carboxylato antimony complexes $[SbAr_3(CO_2^-)_2]$ can be highly effective and selective in their activity towards the parasite promastigotes and amastigotes [25–33]. The Bi(V) analogues tend to have good activity towards the parasites but are generally non-selectively toxic due to the high redox potential and chemical reactivity [26,27].

In contrast to wholly organic drugs, metallodrugs offer the unique characteristic and opportunity of combining biologically active ligands in varying ratios on a metal centre which itself can play a therapeutic role. Alongside this design flexibility they can improve solubility and bioavailability, reduce systemic toxicity, and increase potency [34], and the metal can act specifically as a carrier for bioactive molecules through cellular channels normally inaccessible to the parent organic moiety [35]. Ideally, for a combination drug or therapy the component parts should not have a similar biochemical impact but should be targeting different pathways, functions or structures within the cell [19].

With this in mind, we decided to build on the promising results achieved with $[SbAr_3(CO_2^-)_2]$ complexes and replace the carboxylates moieties with a known class of antimicrobial. To that end we chose the heterocycle 8-quinolinol (8-hydroxyquinoline, 8QH), a planar *N,O* binding phenoxide metal chelator that has been shown to exhibit antimicrobial activity, especially in the presence of metal ions [36–38]. Several organometallic complexes of 8QH have previously been studied for their potential as anti-cancer drugs and as anti-bacterial agents [39,40]. 8QH has also been tested individually against several strains of *leishmania* and shown to exhibit significant activity [41]. The 5,7-halido substituted derivatives of 8QH (Fig. 2) have exhibited medical potential, though in some cases exhibited problems with mammalian toxicity [42–46]. The mechanism of action of this class of heterocycle was determined to rely more on the depolarisation of the parasitic membrane rather than the induction of reactive oxygen species (ROS) or nitric oxide (NO) [47]. As the frontline antimonials elevate both ROS and NO, inducing oxidative stress and therefore apoptosis [48], the combination of these different modes of action is desirable.

As a result of this study six novel heteroleptic triphenyl Sb(V) *mono*-hydroxy *mono*-quinolinolate complexes (Fig. 3) have been synthesised and fully characterised: $[SbPh_3(C_9H_6NO)(OH)]$ 1, $[SbPh_3(C_9H_5NOCl)(OH)]$ 2, $[SbPh_3(C_9H_5NOCl_2)(OH)]$ 3, $[SbPh_3(C_9H_4NOBr_2)(OH)]$ 4, $[SbPh_3(C_9H_4NOI_2)(OH)]$ 5 and $[SbPh_3(C_9H_3NOCl_2CH_3)(OH)]$ 6, and assessed for their activity towards *L. major* promastigotes and amastigotes, and human primary fibroblasts to establish mammalian cell toxicity.

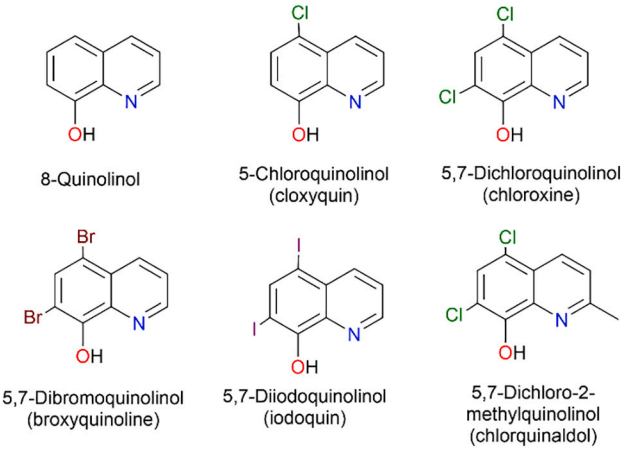

Fig. 2. Six 8-quinolinols used in this study: 8-Qunolinol, $[C_9H_6NO]$; 5-Chloroquinolinol, $[C_9H_5NOCl]$; 5,7-Dichloroquinolinol, $[C_9H_4NOCl_2]$; 5,7-Dibromoquinolinol, $[C_9H_4NOBr_2]$; 5,7-Di-iodoquinolinol $[C_9H_4NOI_2]$; 5,7-Dichloromethylquinolinol $[C_9H_3NOCl_2CH_3]$.

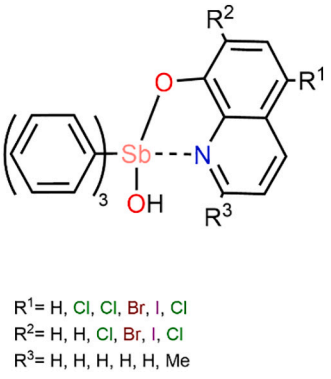

Fig. 3. Generic structure of the six antimony complexes: $[SbPh_3(C_9H_6NO)(OH)]$ 1, $[SbPh_3(C_9H_5NOCl)(OH)]$ 2, $[SbPh_3(C_9H_5NOCl_2)(OH)]$ 3, $[SbPh_3(C_9H_4NOBr_2)(OH)]$ 4, $[SbPh_3(C_9H_4NOI_2)(OH)]$ 5 and $[SbPh_3(C_9H_3NOCl_2CH_3)(OH)]$ 6.

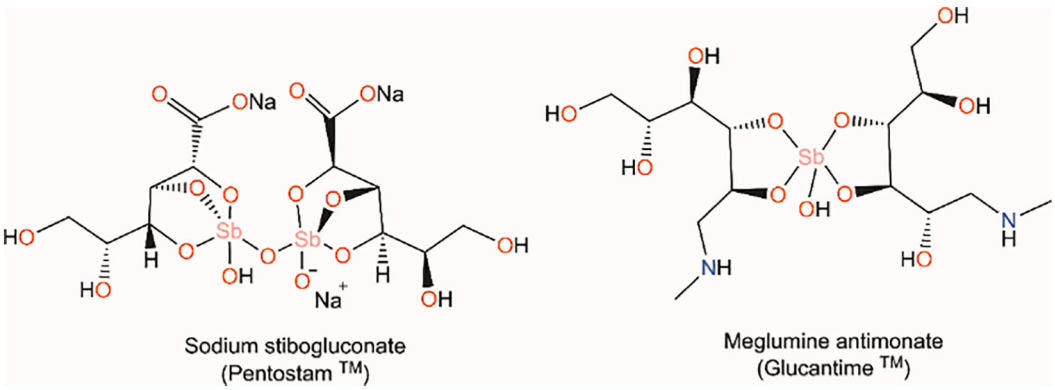

Fig. 1. Current Sb(V) drugs used to treat Leishmaniasis.

2. Experimental

$SbPh_3$ was purchased from Sigma-Aldrich with no need for further purification. All quinolinols were purchased from Sigma-aldrich or alfa Aesar. 5-Chloroquinolniol was purified by crystallisation in hot toluene. Luperox™ (tert-butyl hydroperoxide 70% solution) was purchased from Sigma-Aldrich. All remaining solvents were purchased from Merck. A Bruker Avance DRX600 spectrometer (600 MHz) was used to record the ^{13}C NMR and ^{1}H NMR spectra of all the complexes in deuterated dimethyl sulfoxide (d_6-DMSO). The multiplicities have been denoted as followed: singlet (s), doublet (d), triplet (t), multiplet (m), broad (br) or a combination of two or more. Infrared spectra were recorded on an Agilent Technologies Cary 630 FTIR spectrometer with a range of 4000–500 cm^{-1} given. Melting point analysis was obtained in open end capillary tubes on a SMP10 Stuart Digital Scientific apparatus. Elemental analysis (CHNS) was conducted by the Campbell Microanalytical laboratory, department of Chemistry, University of Otago, Dunedin New Zealand.

2.1. Biological assays

2.1.1. Cell culture

Human primary fibroblasts and J774 macrophages were cultured in Dulbecco's Modified Eagles Medium (DMEM) previously supplemented with 1% GlutaMax™, 1% Pen-Strep and 10% Fetal Bovine Serum (FBS). The cells were maintained at 37 °C in a 5% CO_2 incubator. Virulent clone v121 of *Leishmania major* was derived from the LRC-L137 *L. major* isolate. The parasite was cultured in M199 media supplemented with 1% Pen-Strep, 10% FBS and 7.5 mg/L of haemin in basified H_2O, in a 26 °C incubator [30]. All media and supplements were purchased from Gibco™ and maintained as directed.

2.1.2. In vitro testing of L. major and Human primary fibroblasts

All compounds 1–6 were dissolved into DMSO to 10 mM working stock solutions. The stock solutions were then diluted with the appropriate culture media to 100 μM before serial dilution in duplicate 96 well Falcon plates (100 μM to 48 nM). Volumes of 10^6 promastigotes/mL and 10^5 fibroblasts/mL were added along with Celltiter Blue cell Viability assay, purchased from Promega ™. Plates were incubated for 48 h and then spectroscopically measured using fluorescence excitation at 544 nm and emission at 590 nm. This was compared against a positive control of untreated cells to determine the percentage inhibition [49]. All fluorescence excitation and emission measurements were conducted on a BMG-Labtech ClarioStar Omega microplate reader [50,51]. All errors bars were calculated using the standard error of the replicates.

2.1.3. Amastigote invasion assay

Macrophage invasion assays were performed as previously described. J774 macrophages were plated in a 24 well Falcon plate onto glass coverslips. After 48 h the cells had adhered, they were exposed to *L. major* promastigotes at a 1:5 ratio and incubated for a further 24 h to allow for differentiation into amastigotes. The coverslips were washed to remove any excess promastigotes and then exposed to the complexes for 48 h. After a Giemsa staining the coverslips were mounted using DPX and the cells counted microscopically. From this the percentage of infected cells could be determined using a Dunnetts multiple comparison test against a positive control [52].

2.1.4. Griess assay

J774 macrophages were seeded at 10,000 cells per well in a 24-well plate. The cells were given 24 h to adhere to the plate before infection with 5× the amount of *L. major* promastigotes. The parasites were given 6 h to enter the cells before washing of any excess parasites with PBS. Parasites were given 24 h to differentiate into amastigote. The plate was washed again with PBS to remove any free-floating parasites. Compounds 2 and 5 along with amphotericin B were added in triplicate at a concentration of 10 μM in colourless RPMI. The plate was incubated for a further 6 h. The RPMI was then plated into a 96-well plate and analysed as per the Griess assay protocol [53]. The absorbance was read at 530 nm on a BMG-Labtech ClarioStar Omega microplate reader and the values compared to a standard curve of nitrite to determine the increase percentage of nitric oxide.

2.1.5. Measurement of reactive oxygen species

Measurement of ROS was achieved by a modified assay from Wojtala *et al* [54]. J774 macrophages were plated into 24-well plates at 30,000 cells per well. Cells were given 24 h to adhere before infection with *L. major* promastigotes at 5× the amount in colourless RPMI. The *L. major* promastigotes were incubated for six hours to infect and differentiate into amastigotes before excess promastigotes were washed away with PBS. The cells were incubated for a further 24 h to allow complete infection. Complexes 2, and amphotericin B were added to wells in triplicate at a concentration of 10 μM. A positive control of infected cells without drug treatment was included. At intervals of 6, 24 h, 1 μM of DHE was added and the plate incubated for a further 200 minutes in the absence of light. After this, the cells were washed with PBS and a fluorescence reading taken in the measurement buffer of 5 mM of glucose in PBS at excitation of 535 nm and emission of 635 nm on a BMG-Labtech ClarioStar Omega microplate reader. Treated wells were compared to the positive control and the percentage increase calculated.

2.1.6. X-ray crystallography

Crystallographic data for compound 1 was collected on an OXFORD XtaLAB Synergy, Dualflex, HyPix diffractometer equipped with an OXFORD Cryosystems 700 Cryostream and cooled to 123(10) K. Data was collected with monochromatic MoK_α radiation ($\lambda = 0.71070$ Å) and processed using the CrysAlisPro v 1.171.40.49a software [55]. Crystallographic data on compounds 4–6 were collected on a Bruker X8 APEXII CCD diffractometer, equipped with an OXFORD Cryosystem 700 cryostream and cooled to 123(2) K. Data collection occurred using monochromatic (graphite) MoK_α radiation ($\lambda = 0.71070$ Å) and were processed using the Bruker Apex2 v2014.7–1 software [56], polarisation, Lorentz and absorption corrections (multi-scan-SADBABS) were applied [57]. Each compound was solved and refined using SHELXL-2014/7 utilising the graphical interface X-Seed or Olex2 with the final refinement done in Olex2 alone [57–59]. Unless otherwise indicated, all non-hydrogen atoms were refined with anisotropic thermal parameters. Hydrogen atoms were placed in calculated positions using a riding model with C-H = 0.95–0.98 Å and $U_{iso}(H) = xU_{iso}(C)$, $x = 1.2$ or 1.5 unless otherwise indicated. Hydrogen atoms of the O—H groups were placed in calculated positions based on the bond lengths of the oxygen atom. Crystallographic data of complexes 2 and 3 were collected at the MX1 beamline at the Australian Synchrotron, Melbourne, Victoria, Australia, operating at 17.4 KeV, with $\lambda = 0.7073$ Å, using an open flow N_2 cryostream cooled to 123(2) K. The data collection and reduction was obtained using BlueIce, [59] and XDS [60]. Disorder of the DMSO molecule in compound 6 was modelled over two positions.

2.2. Synthesis and characterisation

2.2.1. General procedure

1 mmol of $SbPh_3$ was dissolved into toluene and 2 equivalents of 70% t-BuOOH in water solution (Luperox™) added. The clear solution was stirred for 10–15 min before addition of 1 mmol of the corresponding substituted 8-quinolinol. An immediate colour change was observed from colourless to yellow. The solution was stirred overnight before removal of the solvent, water and tert-butanol by-products under reduce pressure. Yellow–green solids were obtained after sonication of the resultant oils in water. Crystals of each complex were grown from slow evaporation of the solid in toluene or DMSO solvent.

Triphenylantimony mono-hydroxy 8-quinolinolate, 1. $SbPh_3$ (0.353 g, 1 mmol) was reacted with t-BuOOH (140 μL, 2 mmol) before addition of 8-

quinolinol (0.145 g, 1 mmol) according to GP2. Yellow solid (0.427 g, 83%). m.p: 161–162 °C; ^{1}H NMR (400 MHz, DMSO-d_6) δ = 9.10 (dd, J = 4.6, 1.4 Hz, 1H), 8.40 (dd, J = 8.4, 1.4 Hz, 1H, CH_{ar}), 7.73–7.65 (m, 6H, CH_{ar}), 7.65–7.57 (m, 1H, CH_{ar}), 7.52–7.43 (m, 1H, CH_{ar}), 7.23–7.14 (m, 9H, CH_{ar}), 7.11 (ddd, J = 12.8, 8.0, 1.2 Hz, 2H, CH_{ar}), 4.78 (s, 1H, OH). ^{13}C NMR (101 MHz, DMSO-d_6) δ = 156.4 (SbC), 142.1 (C_{ar}), 139.3 (C_{ar}), 130.0 (C_{ar}), 129.7 (C_{ar}), 128.9 (C_{ar}), 128.4 (C_{ar}), 127.9 (C_{ar}), 121.2 (C_{ar}), 113.9 (C_{ar}), 104.5 (C_{ar}); FT-IR [cm $^{-1}$]: 3571 (w), 2109 (w), 1575 (m), 1495 (m), 1460 (sh), 1429 (m), 1390 (m), 1319 (sh), 1279 (m), 1239 (w), 1103 (sh), 1064 (m), 824 (m), 735 (sh). 692 (sh); Elemental analysis: Expected: C:63.06H:4.31 N:2.72 Found: C:63.35H:4.48 N:2.71 CCDC: 1942090.

Triphenylantimony mono-hydroxy 5-chloro-8-quinolinolate, 2. $SbPh_3$ (0.353 g, 1 mmol) was reacted with t-BuOOH (140 µL, 2 mmol) before addition of 5-chloro-8-quinolinol (0.179 g, 1 mmol) according to GP2. Yellow solid (0.448 g, 81%). m.p: 128–130 °C; ^{1}H NMR (600 MHz, DMSO-d_6) δ = 9.18 (dd, J = 4.6, 1.4 Hz, 1H, CH_{ar}), 8.51 (dd, J = 8.5, 1.4 Hz, 1H, CH_{ar}), 7.79 (dd, J = 8.5, 4.6 Hz, 1H, CH_{ar}), 7.71–7.66 (m, 6H, CH_{ar}), 7.60 (d, J = 8.4 Hz, 1H, CH_{ar}), 7.27–7.13 (m, 9H, CH_{ar}), 7.09 (d, J = 8.5 Hz, 1H, CH_{ar}), 4.95 (s, 1H, OH); ^{13}C NMR (101 MHz, DMSO-d_6) δ = 156.2 (SbC), 151.0 (C_{ar}), 143.1 (C_{ar}), 135.6 (C_{ar}), 132.8 (C_{ar}), 129.9 (C_{ar}), 128.6 (C_{ar}), 126.8 (C_{ar}), 123.1 (C_{ar}), 114.4 (C_{ar}); FT-IR [cm $^{-1}$]: 3241 (br), 3052 (w), 2109 (w), 1571 (m), 1492 (m), 1452 (sh), 1429 (m), 1379 (m), 1362 (s) 1308 (sh), 1256 (m), 1084 (w), 1022 (sh), 826 (m), 740 (sh), 697 (sh); Elemental analysis (2.dmso), Expected: C:55.57H:4.34 N:2.23 S:5.11 Found: C:55.40H:4.38 N:2.22 S:5.02. CCDC: 1901551.

Triphenylantimony mono-hydroxy 5,7-dichloro-8-quinolinolate, 3. $SbPh_3$ (0.353 g, 1 mmol) was reacted with t-BuOOH (140 µL, 2 mmol) before addition of 5,7-dichloro8-quinolinol (0.214 g, 1 mmol) according to GP2. Yellow solid (0.594 g, 89%). m.p: 95–97 °C; ^{1}H NMR (600 MHz, DMSO-d_6) δ = 9.20 (dd, J = 4.6, 1.4 Hz, 1H, CH_{ar}), 8.49 (dd, J = 8.5, 1.4 Hz, 1H, CH_{ar}), 7.83 (s, 1H, 7.77 (dd, J = 6.2, 4.4 Hz, 6H, CH_{ar}), 7.31–7.10 (m, 10H, CH_{ar}), 5.16 (s, 1H, OH^{13}C NMR (101 MHz, DMSO) δ 152.2 (SbC), 151.9 (C_{ar}), 144.5 (C_{ar}), 136.1 (C_{ar}), 135.6 (C_{ar}), 132.6 (C_{ar}), 129.5 (C_{ar}), 128.8 (C_{ar}), 128.3 (C_{ar}), 125.7 (C_{ar}), 123.1 (C_{ar}), 118.1 (C_{ar}), 114.7 (C_{ar}); FT-IR [cm $^{-1}$]: 3244 (w), 3053 (w), 2165 (w), 1571 (m), 1494 (m), 1450 (sh), 1429 (m), 1397 (m), 1308 (sh), 1256 (w), 1084 (m), 1025 (sh), 958 (sh), 826 (m), 740 (sh), 697 (sh); Elemental analysis (3.2H_2O) Expected: C:52.38H:3.91 N:2.26 Found C:52.61H:4.06 N: 2.27. CCDC: 1938022.

Triphenylantimony mono-hydroxy 5,7-dibromo-8-quinolinolate, 4. $SbPh_3$ (0.353 g, 1 mmol) was reacted with t-BuOOH (140 µL, 2 mmol) before addition of 5,7-dibromo-8-quinolinol (0.303 g, 1 mmol) according to GP2. Yellow solid (0.540 g, 72%). m.p: 121–123 °C; ^{1}H NMR (600 MHz, DMSO-d_6) δ = 9.17 (dd, J = 4.6, 1.4 Hz, 1H, CH_{ar}), 8.41 (dd, J = 8.5, 1.4 Hz, 1H, CH_{ar}), 8.05 (s, 1H, CH_{ar}), 7.82–7.71 (m, 6H, CH_{ar}), 7.29–7.12 (m, 10H, CH_{ar}), 5.16 (s, 1H, OH); ^{13}C NMR (101 MHz, DMSO-d_6) δ = 150.4 (C_{ar}), 138.0 (C_{ar}), 132.6 (C_{ph}), 128.9 (C_{ph}), 128.3 (C_{ph}), 127.3 (C_{ar}), 123.5 (C_{ar}), 104.5 (C_{ar}); FT-IR [cm $^{-1}$]: 3275 (w), 3065 (w), 2081 (w), 1560 (m), 1481 (m), 1430 (sh), 1390 (m), 1357 (sh), 1309 (m), 1242 (w), 1103 (m), 1022 (sh), 943 (m), 864 (w), 743 (sh), 690 (sh); Elemental analysis (4.dmso), Expected: C:46.43H:3.49 N:2.03 S:4.27 Found: C:46.30H:3.49 N:1.87 S:4.42. CCDC: 1938252.

Triphenylantimony mono-hydroxy 5,7-diiodo-8-quinolinolate, 5. $SbPh_3$ (0.353 g, 1 mmol) was reacted with t-BuOOH (140 µL, 2 mmol) before addition of 5,7-diiodo-8-quinolinol (0.397 g, 1 mmo). Yellow solid (0.598 g, 78%) according to GP2. m.p: 179–181 °C; ^{1}H NMR (400 MHz, DMSO-d_6) δ = 9.10 (dd, J = 4.6, 1.4 Hz, 1H, CH_{ar}), 8.31 (s, 1H, CH_{ar}), 8.27 (dd, J = 8.5, 1.3 Hz, 1H, CH_{ar}), 7.75 (dd, J = 8.5, 4.5 Hz, 6H, CH_{ar}), 7.21 (m, 10H, CH_{ar}), 5.12 (s, 1H, OH); ^{13}C NMR (101 MHz, DMSO-d_6) δ = 132.5 (C_{ph}), 128.7 (C_{ph}), 128.2 (C_{ph}); FT-IR [cm $^{-1}$]: 3050 (w), 2115 (w), 1545 (m), 1475 (m), 1430 (sh), 1385 (m), 1353 (sh), 1307 (w), 1243 (m), 1102 (m), 1063 (m), 846 (m), 733 (sh), 692 (sh); Elemental analysis, Expected: C:41.47H: 2.54 N:1.86 Found: C:41.38H:2.75 N:1.89. CCDC: 1938021.

Triphenylantimony mono-hydroxy 5,7-dichloro-2-methyl-8-quinolinolate, 6. $SbPh_3$ (0.353 g, 1 mmol) was reacted with t-BuOOH (140 µL, 2 mmol) before addition of 5,7-dichloro-2-methyl-8-quinolinol (0.229 g, 1 mmol) according to GP2. Yellow solid (0.449 g, 75%). m.p: 150–153 °C; ^{1}H NMR (600 MHz, DMSO-d_6) δ = 8.23 (d, J = 8.6 Hz, 1H, CH_{ar}), 7.88 (dt, J = 6.3, 1.4 Hz, 6H, CH_{ar}), 7.71 (s, 1H, CH_{ar}), 7.42 (d, J = 8.6 Hz, 1H, CH_{ar}), 7.31–7.21 (m, 10H, CH_{ar}), 4.93 (s, 1H, OH), 2.91 (s, 3H, CH_3). ^{13}C NMR (101 MHz, DMSO-d_6) δ = 137.1 (C_{ar}), 134.3 (C_{ar}), 132.6 (C_{ph}), 129.2 (C_{ph}), 129.4 (C_{ph}), 104.5 (C_{ar}); FT-IR [cm $^{-1}$]: 3599 (w), 3048 (w), 2973 (w), 1573 (w), 1548 (w), 1480 (w), 1423 (sh), 1357 (m), 1326 (m), 1251 (w), 1107 (m), 1021 (w), 829 (m), 732 (sh). 690 (sh); Elemental analysis (6sq.tBuOH), Expected: C:57.26H:4.84 N:2.17 Found: C:57.48H:447 N:2.30. CCDC: 1938023.

3. Results and discussion

3.1. Synthesis and characterisation

The antimony complexes 1–6 were synthesised through an oxidative addition reaction. Triphenyl antimony was first oxidised from +III to +V by the addition of two equivalents of *tert*-butyl hydroperoxide, before addition of the desired quinolinol (Scheme 1), using a modified version of a synthesis first reported by Moiseev *et al* [61]. The by-products produced, tBuOH and H_2O, are easily removed under vacuum. The resultant yellow oils were sonicated in water to produce yellow/green solids. The initial targets were the triphenyl Sb(V) *bis*-quinolinolato complexes, [$SbPh_3L_2$], through the use of two equivalents of quinolinol (LH). However, analysis of the ^{1}H NMR spectra indicated that only the *mono*-quinolinolato complexes, [$SbPh_3$(OH)L], are formed irrespective of the stoichiometry (Scheme 1).

Using the appropriate 1:1 stoichiometry allows for the isolation of clean products in good yield (72–90%) with minimal workup. Crystals of complex 2–6 were each obtained through slow evaporation in DMSO solution. The crystal structures thereby obtained show that, with the exception of 1, the crystals incorporate DMSO in the interstices interacting through hydrogen bonding with the hydroxyl ligand covalently bound to the metal centre. In contrast, the structure of 1 indicates direct hydrogen bonding through hydroxyl ligands on two molecules. These structural features are discussed in the X-ray crystallographic section below. The solid-state structures correlate well with the respective ^{1}H NMR spectra.

These complexes are the first example of heteroleptic triphenyl antimony (V) *mono*-hydroxido *mono*-quinolinolato complexes. The only other relevant study of a closely related complex is that of the triphenyl *mono*-chlorido complex of 8-quinolinolate [62]. All analytical data supports the complexes having the composition [$SbPh_3$(OH)L].

In summary, the ^{1}H and ^{13}C NMR spectra of each complex were obtained in d_6-DMSO. Complexation of the quinolinolate to the metal centre is characterised by the lack of the hydroxyl signal from the parent quinolinol normally observed in 9.78–11.05 ppm range. A shift in both the aromatic signals of the quinolinol and the parent $SbPh_3$ is observed to higher frequencies, consistent with that observed for previously synthesised *tris*-aryl Sb(V) complexes [25]. All data can be found in the

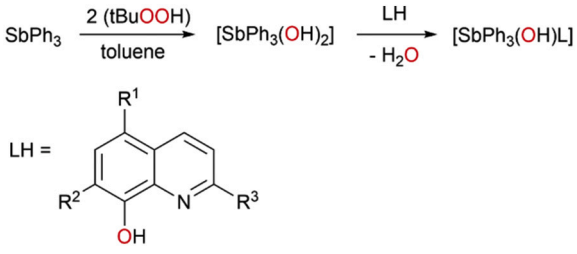

Scheme 1. Oxidative addition reaction resulting in the Sb(V) *mono*-quinolinolato complexes 1–6.

ESI.

The FT–IR spectrum of each complex provided additional information on the binding of the quinolinolate ligand through a shift in the broad O—H signal from ~3300 to 2800 cm^{-1} in each of the complexes. It was also found that a significant shift in the strong C—N signal, ranging from 1201 to 1190 cm^{-1}, and the OH bend ranging from 1331 to 1276 cm^{-1}, in the parent quinolinols was observed in the complexes. A weak, broad signal was observed for the covalently bound hydroxyl in the complexes in the range 3306–3241 cm^{-1}. The IR spectrum for each complex can be found in the ESI along with a table detailing specific absorbances (Table S1).

3.1.1. X-ray crystallography

Crystal of all six complexes were analysed using single crystal X-ray diffraction. A summary of the X-ray data for all complexes 1–6 can be found in the ESI. The geometry of the compounds can be described as distorted octahedral. All compounds were found to deviate from the ideal 180 ^{o} angle along the axial plane of the deprotonated quinolinol and covalently bound hydroxyl (O—Sb—O), with a range of 164.3^{o}–174.0^{o}. Compound 6 was found to exhibit the largest degree of distortion and compound 2 the least. This may be due to the additional steric effects of halides at both the five and seven position and the added methyl group at the two position for the quinolinol ligand of compound 6. Compounds 1 and 5 will be discussed in more detail (Fig. 4). Compound 1 was the only compound that did not require a hydrogen bonded solvent molecule for crystallisation, it was instead found to self-associate with a second moiety in the asymmetric unit to form a dimer (Fig. 4).

The Sb—O distances of 2.105(2), 2.066(2) and 1.984(2), 2.010(2) both for Sb(1)—O(1), Sb(1A)—O(1A) and Sb(1)—O(2), Sb(1A)—O(2A) respectively, are described as covalent in nature and along with the two sets of three Sb—C interactions (Sb(1)—C(10), 2.161(3) Å, Sb(1A)—C(10A), 2.151(3) Å, Sb(1)—C(16), 2.143(3) Å, Sb(1A)—C(16A), 2.150(3) Å and Sb(1)—C(22), 2.145(3) Å, Sb(1A)—C(22A), 2.149(3) Å) balance the charge of each Sb(V) centre. Bond angles for the C—Sb—C of the phenyl rings of 169.2(12) ^{o}, 95.98(12) ^{o} and 94.79(12) ^{o} for C(22) – Sb(1) – C(10), C(16)—Sb(1)—C(22) and C(16)—Sb(1)—C(10) and 163.9(12) ^{o}, 96.22(12) ^{o} and 99.66(13) ^{o} for C(22A)—Sb(1A)—C(10A), C(16A)—Sb(1A)—C(22A) and C(16A)—Sb(1A)—C(10A), respectively, are not dissimilar to the angles observed in the pentacoordinate Sb(V) *tris*-aryl carboxylates previously synthesised [26,33,27]. This give the phenyl rings an overall propeller-like orientation with is characteristic of *tris*-aryl Sb(V) complexes [26,28,29,63–69]. The remaining axial positions are occupied by the oxygen moieties of the hydroxyl and quinolinol. The datively bound nitrogen (bond range of 2.389 Å—2.597 Å for compounds 1–6) occupies the remaining equatorial position. The bulk representative example 5 (Fig. 4), is analogous in structure to the remaining compounds.

Like compound 1, it is six-coordinate distorted octahedron. A similar configuration was observed in previously reported complexes [26,70]. As mentioned previously, distortion along the O—Sb—O angle from the ideal 180 ^{o} is reported.

Coordination of the N atom is confirmed by the Sb—N bond length of 2.389(4). This is similar to those described by Hoskins *et al* for a *bis*-quinolinolato Sb(III) (Sb—N distances of 2.368(7) and 2.373(7) Å), and a tetranuclear complex synthesised by Jami and Baskar, which exhibits a short Sb—N coordinate bond length of 2.238(2) Å [71,72]. The Sb—O bond distance for the quinolinolato ligand, at 1.967(4) Å is shorter than the respective Sb—O bonds involving the hydroxide (2.118(3) Å (5)). These lengths are well within the typical range of a covalent interaction of Sb—O bonds [73,74]. Interestingly the bond angle for the OH—O interaction of each complexes was found to increase from 1 to 5, with compound 6 the outlier. This may be due to the increase of halide size on the quinolinol moiety, with the larger halides causing a larger inductive effect on the complex as a whole.

3.2. Stability studies

3.2.1. Solid and solution state analysis

The stability of the six complexes in both the solid and solution states was determined over a minimum period of one month. With respect to solid-state stability, melting point analysis showed no change for each of the complexes over several months of screening. The solution state stability was studied through ^{1}H NMR spectroscopy over a defined period. Each complex was dissolved in deuterated d_6-DMSO, which had not been pre-dried, and a spectrum recorded at 0 and 24 h. No observable changes in the chemical shifts occurred, suggesting a high degree of stability towards ligand rearrangement and hydrolysis. All of the spectra can be found in the ESI.

3.2.2. Stability in cell culture media

To understand whether the complex as constituted is the antimicrobial agent, then a high degree of stability in culture media is required. Previous studies on *tris*-aryl Bi(V) carboxylates have shown that the degree of stability in culture media can vary. For example, we previously reported that triphenyl and *tris*-tolyl Bi(V) NSAID complexes exhibit rapid exponential decay in culture media (NSAID = non-steroidal anti-inflammatory drug) [30,31]. In contrast, the analogous Sb(V) complexes were all found to exhibit a high degree of stability in media with cell selectivity [25–27].

Complex 2, [$SbPh_3(C_9H_5NOCl)(OH)$] was used as an exemplar to understand the stability of the complexes in media. The complex was dissolved in d_6-DMSO at a concentration of 10 mM. From this stock 100 μL was suspended into 900 μL of D_2O suspended DMEM. At this concentration a small degree of precipitation occurred. A ^{1}H NMR was taken at times 0, 6, 12, 18 and 24 h to determine culture media stability. The protons on the Ph groups were able to be distinguished easily. Signals in

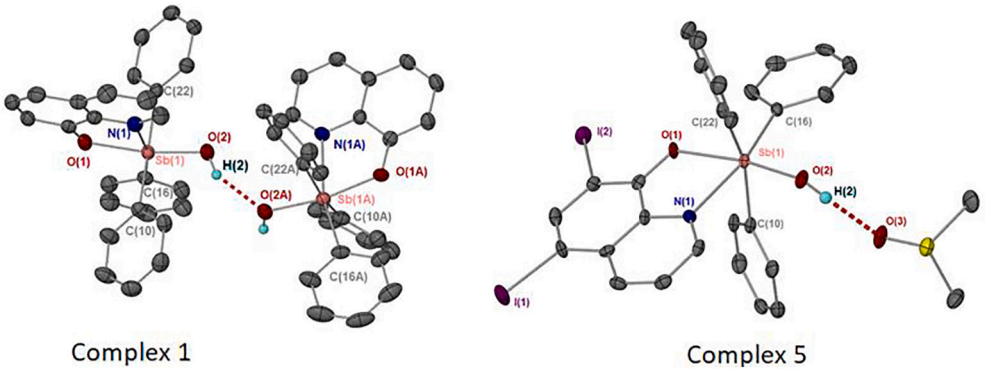

Fig. 4. Solid-state structure of complex 1, 2[$SbPh_3(C_9H_6NO)(OH)$] and complex 5, [$SbPh_3(C_9H_4NOI_2)(OH)$]. Thermal ellipsoids at 50% probability. Hydrogen atoms except for those that are relevant have been omitted for clarity. Selected bond lengths (Å and angles (^{o}) can be found in the ESI.

relation to the quinolinolate moiety remained close the baseline and because of the lower number of protons relative to those of Ph were difficult to assign. A control spectrum of $SbPh_3$ in culture media was used to determine that the complex had not undergone reduction into $SbPh_3$ and parent quinolinol (Fig. 5).

A consistent signal from the culture media at 5.10 ppm was set to an integral value of 1.00 and its ratio to one of the aromatic protons of complex 2 at 7.90 ppm compared at each time point. No significant changes to the integration was detected over the 24-h period, indicating a high degree of DMEM stability (Fig. 6).

3.3. Biological activity

3.3.1. Leishmania promastigote and mammalian cytotoxicity

8-Quinolinol (8-hydroxyquinoline) is known to act as an anti-leishmanial agent, and can exhibit increased bactericidal effects in the presence of metal ions. It was hypothesised that incorporating the quinolinolate anion into an aryl-Sb(V) complex could generate a positive additive or synergistic effect [36,38,41]. As such, all the Sb(V) complexes 1–6 were assessed for their activity towards both *L. major* promastigotes and the more clinically relevant amastigote form. Mammalian cytotoxicity was assessed using human primary fibroblasts. Each complex was examined using a Celltiter blue viability assay against both *L. major* promastigotes and human fibroblasts, with each assay duplicated and an average of these repeats plotted.

All complexes exhibited excellent activity against the promastigote form, with IC_{50} values ranging from 2.03–3.39 μM (Fig. 7). Amphotericin B and DMSO were tested as controls and the data can be found in ESI Figs. S2 and S3. Complex 6 proved to be the most potent of the complexes, though there is no clear and obvious trend arising from the change in halide and ring position. The level of anti-promastigote activity of these complexes surpasses that found in our previous studies with triphenyl Sb(V) acetates, with the most effective of those complexes presenting with an IC_{50} value of 6.18 μM [27]. The lability of the aryloxido—metal bond, and hence the release kinetics of the quinolinol, may contribute to this increased activity, since carboxylates are more anionic ligands and less labile [75,76].

Each complex 1–6 was found to exhibit toxicity towards to human fibroblasts within the range of 12.7–46.9 μM (Fig. 8) with $[SbPh_3(C_9H_6NO)(OH)]$ 1 the most toxic and $[SbPh_3(C_9H_4NOI_2)(OH)]$ 5 the least. Interestingly, a trend became apparent whereby an increase in the size of the halide results in a decrease in mammalian cell toxicity. Complexes 5 and 4, respectively, are the most selective of the series, though 1, 2 and 3 displayed reasonable selectivity indices, due to their potency on *L. major* promastigotes. Selectivity indices have been calculated in the ranges of 4.52–16.7, and are shown below in Table 1. ClogP values were calculated showing that an increase in halide size correlates to an increase of the ClogP. This increase of ClogP seemed to also correlate to an increase in selectivity, indicating an interesting structure-activity relationship.

Complexes 4, 5 and 6 in particular show good selectivity, with a 16-fold increase from mammalian to parasite IC_{50}. Even the remaining complexes still fall above the range of the FDA definition of a narrow therapeutic index (2-fold increase mammalian, microbe), indicating their potential in future assays [77].

3.3.2. Amastigote invasion assay

An amastigote invasion assay was undertaken on complexes 1–6. Amastigotes are the mammalian infective form of the parasite, therefore activity against this stage is imperative for any potential anti-leishmanial [78]. Each complex was found to exhibit excellent activity at the standard concentration of 10 μM (Fig. 9). The percentage infection values ranged from 2.25%–9.00%. Similar to the cytotoxicity studies on fibroblasts, an increase in halogen size on the 5 and 7 positions lead to an increase in anti-amastigote activity. Complex 5 $[SbPh_3(C_9H_4NOI_2)(OH)]$ proved the most efficient in eradicating infection (2.25% ± 0.25), with the dichlorquinolinolate complex, 6 $[SbPh_3(C_9H_4NOCl_2CH_3)(OH)]$ proving the least effective (9.00% ± 0.83). Despite this, all complexes exhibited a greater degree of activity (Table 2) than recently studied triphenyl Sb(V) carboxylate complexes (percentage infection range, 9.50%–30.0% [26], 7.75%–40.5% [27]). In fact, the range of percentage infection for these quinolinolate complexes was observed to be much lower than the previously examined bis-carboxylates, with less variation in their activity for all six compounds.

Each of the parent quinolinols was also assessed for its anti-leishmanial activity. Previous studies on 8QH showed it to be potent against three separate leishmanial strains (*L. amazonensis*, *L. braziliensis* and *L. infantum)* but only at a relatively high concentration of 68 μM [41]. In this study all the parent quinolinols display anti-leishmanial activity at the comparison concentration of 10 μM but exhibit lower activity than their corresponding antimony complex at the same concentration. (Table 2, Fig. S4). Thus, the metal complex is more effective than the quinolinol alone and the combination of the triphenyl Sb moiety and the quinolinolate ligand have provided better results than the carboxylate analogues we have studies.

Overall, taking into consideration the selectivity and anti-amastigote activity, complex 5, the iodoquin complex, looks to be best lead compound from this series. Further structural modification in the aryl groups and quinolinols, and future *in vivo* testing would allow further clarification of the potency of these complexes as anti-leishmanial agents.

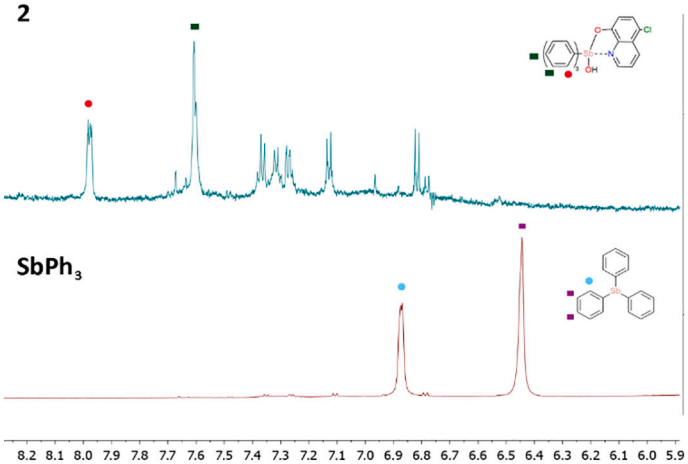

Fig. 5. Comparative ^1H NMR spectra of $SbPh_3$ and 2, $[SbPh_3(C_9H_5NOCl)(OH)]$, in D_2O DMEM. Signals in relation to the culture media at 7.37, 7.32, 7.28, 7.12 and 6.82 ppm have not been labelled on either spectrum.

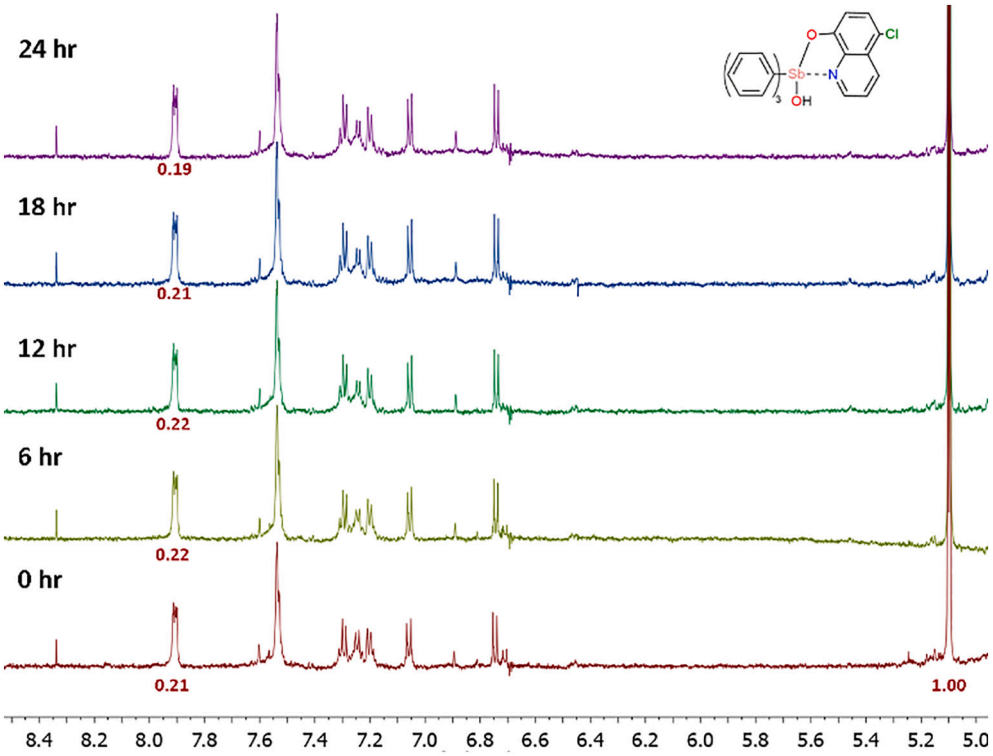

Fig. 6. ^{1}H NMR study of complex 2, [$SbPh_3(C_9H_5NOCl)(OH)$], in DMEM culture media at 0, 6, 12, 18 and 24 h, at 25 °C. Signals in the culture media in the aromatic region have not been labelled. Integration ratio calculated using the culture media signal at 5.10 ppm as the control.

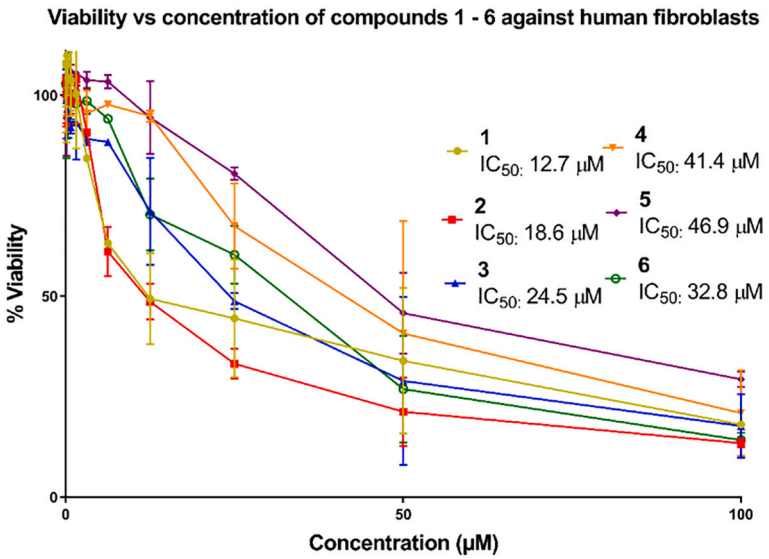

Fig. 7. Comparison of percentage cell viability after treatment with the Sb(V) complexes 1–6, against Human fibroblasts. Dose response curves were generated over a range of concentrations (48 nm–100 μM) in the appropriate culture media from 10 mM DMSO stock solutions. All readings were compared spectroscopically to non-treated control and the percent growth inhibition calculated. A DMSO control and positive drug control (Amp B) were also included at the same range of concentrations which can be found in the ESI (S2 and S3).

3.3.3. *Measurements of reactive oxygen species and nitric oxide*

Leishmania species are able to avoid host immunity by decreasing and inhibiting the production of both reactive oxygen species (ROS) and nitric oxide (NO), two major constituents of the macrophage's immune response [79–83]. To probe a potential mechanism of action of these active antimony complexes two further assays were performed to measure the production of ROS and NO. A Griess assay was performed on infected macrophages that had been exposed to two example complexes, 2, a low SI complex, and 5, which was highly potent to amastigotes. A control of amphotericin B was also employed along with infected macrophages with no drug exposure. Similar to a recent study on alkyl gallium quinolinolates, there was no increase in the production of NO observed (ESI, Fig. S5, Table S3) [84]. Studies into the leishmanicidal effects of piperine compounds by Ferreira *et al.* observed a similar response, with a down regulation of NO observed despite being effective anti-leishmanials [85]. Therefore, it can be assumed that the antimony complexes do not cause amastigote death by activation of NO production. Measurement of the generation of ROS was then analysed through exposure to the compounds and controls at 6 and 24 h. Increase of ROS was detected spectroscopically by the addition of the non-fluorescent dye, dihydroethidium. *Leishmania* amastigotes are able to block production of ROS [81,86], therefore if the infection is still relatively high, very little DHE will be oxidised to the fluorescent form. At 6 h exposure, both 2 and 5 were found to induce a high percentage increase of ROS

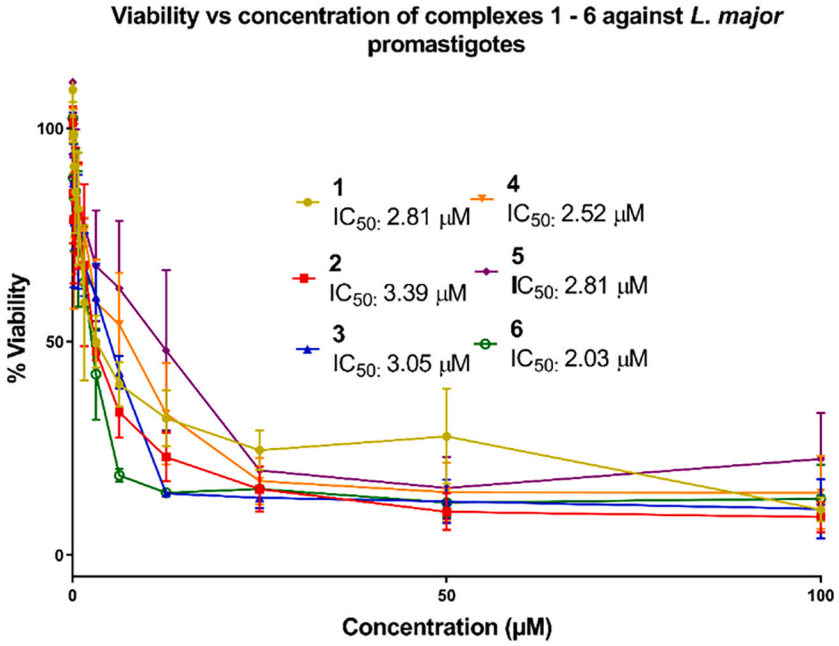

Fig. 8. Comparison of percentage cell viability after treatment with the Sb(V) complexes 1–6, against *L. major* promastigotes. Dose response curves were generated over a range of concentrations (48 nm – 100 μM) in the appropriate culture media from 10 mM DMSO stock solutions. All readings were compared spectroscopically to non-treated control and the percent growth inhibition calculated. A DMSO control and positive drug control (Amp B) were also included at the same range of concentrations which can be found in the ESI (S2 and S3).

Table 1
Selectivity indices of complexes 1–6. Indices calculated based on IC_{50}(mammalian)/IC_{50}(parasite). ClogP values are also listed for comparative purposes.

	Fibroblasts IC_{50} (μM)	Promastigotes IC_{50} (μM)	Selectivity Index	ClogP
1	12.7	2.81	4.52	6.63
2	18.6	3.39	5.49	7.34
3	24.5	3.05	8.03	8.06
4	41.4	2.52	16.4	8.34
5	46.9	2.81	16.7	8.88
6	32.8	2.03	16.2	8.56

when compared to the control of infected cells without treatment, and a greater increase than the drug control amphotericin B. After 24 h the percentage of ROS has dropped dramatically, with a decrease from the control for 2 (ESI Fig. S6, Table 3). This would suggest that activation of ROS plays a major role in the activity of the antimony complexes. The dramatic decrease after 24 h may indicate that these drugs are able to act upon the parasites within this time frame. Pentostam ™ has been shown to induce both NO and ROS production in *Leishmania* infected macrophages through its reductive pathway, therefore it is likely these Sb(V) quinolinolates would share some similar characteristics [48,87].

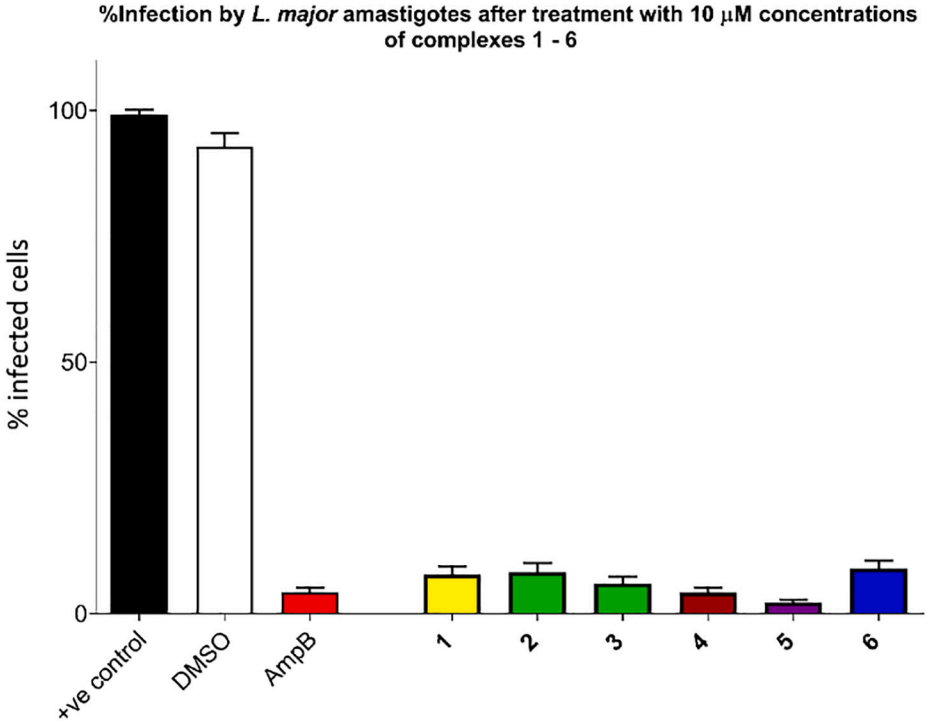

Fig. 9. Infected macrophages after treatment of complexes 1–6, after 48 h. Number of infected macrophages was determined microscopically, in duplicate of fixed specimens. Amphotericin B (AmpB) was used as a positive control at 10 μM concentration. A DMSO control was also employed at a 1% concentration. Error bas indicate SEM, one-way ANOVA. Dunnett's multiple comparison test was used to determine the statistical significance between all test compounds and a positive control lacking treatment (+ve control).

Table 2
Percentage infection values for the parent quinolinols and Sb(V) complexes 1–6, all values are calculated by comparison to a positive control of untreated infected cells.

Quinolinol (LH)	% Infection	Sb(V) complex [$SbPh_3(OH)L$]	% Infection
8 -Quinolinol	15.3 ± 3.00	1	7.75 ± 0.85
5-Chloroquinolinol	21.5 ± 5.13	2	8.25 ± 0.95
5,7-Dichloroquinolinol	30.8 ± 3.28	3	6.00 ± 0.71
5,7-Dibromoquinolinol	23.8 ± 4.86	4	4.25 ± 0.48
5,7-Diiodoquinolinol	16.0 ± 2.81	5	2.25 ± 0.25
5,7-Dichloro-2-methylquinolinol	12.5 ± 2.92	6	9.00 ± 0.83

Table 3
Percentage increase of ROS after exposure to complexes 2 and 5 after 6 and 24 h. The drug control ampB has also been included.

Time (hr)	Complex		Amp B
	1	5	
6	141.8 ± 1.60	153.3 ± 11.7	120.4 ± 2.93
24	82.0 ± 0.31	103.5 ± 2.30	108.8 ± 0.89

4. Conclusions

In seeking to form a new class of potential anti-leishmanial combi-drug we have synthesised and fully characterised six novel triphenyl antimony *mono*-hydroxido *mono*-quinolinolato complexes $[SbPh_3(C_9H_6NO)(OH)]$, 1, $[SbPh_3(C_9H_5NOCl)(OH)]$ 2, $[SbPh_3(C_9H_5NOCl_2)(OH)]$ 3, $[SbPh_3(C_9H_4NOBr_2)(OH)]$ 4, $[SbPh_3(C_9H_4NOI_2)(OH)]$ 5 and $[SbPh_3(C_9H_3NOCl_2CH_3)(OH)]$ 6. Irrespective of reaction stoichiometry only one quinolinolato ligand can be incorporated into the structure leaving one residual hydroxyl group on the Sb(V) centre. The crystal structure of each complex indicates a distorted octahedral coordination environment at Sb(V) with the three Ph groups and the N from the quinolinolate ligand occupying the equatorial plane and the oxygen atoms from the chelating quinolinolate and the hydroxide moiety in the axial positions.

The complexes as solids are stable in air over several months, and are stable towards ligand substitution and hydrolysis in DMSO solution over 24 h but change slowly over seven days. Complex 2, as an exemplar, was found to be stable in DMEM culture media over 24 h.

All the complexes showed some degree of mammalian cell toxicity, with IC_{50} values in the range of 12.7–46.9 μM for human fibroblasts. Despite this, all complexes exhibited an excellent degree of activity against the motile *L. major* promastigotes with an IC_{50} range of 2.03–3.39 μM, providing high selectivity indices 4, 5 and 6. All the complexes showed very good anti-amastigote activity at 10 μM giving % infection values range of 2.25 (5) – 9.00 (6) %. The anti-amastigote activity correlates to an increase in size of the halogen in the 5 and 7 positions: Cl ≤ Br ≤ I for complexes 2 (8.25% ± 0.95), 3 (6.00% ± 0.71), 4 (4.25% ± 0.48) and 5 (2.25% ± 0.25). All the Sb(V) complexes showed greater activity than their corresponding parent quinolinols (range: 12.5%–30.8%). Compounds 4 and 5 were found to be more effective than the drug control Amp B, alluding to their potential in future applications. This study has also shed light into a potential mode of action in relation to the production of reactive oxygen species (ROS) rather than the generation NO. In terms of selectivity and anti-amastigote activity complex 5 present as the most prospective candidate in the class. Overall, the study has found that the combination of two anti-leishmanial moieties (Sb(V) and quinolinol) in a single complex has the potential to be an effective strategy for the development of new combi-drugs.

Author contributions

All contributors involved in drafting and finalisation of manuscript.
Dr Rebekah N. Duffin
Principle research student
– Data curation, formal analysis, Investigation (synthesis and biological assays)
Dr Victoria L. Blair
Research Fellow
– Investigation, Supervision and Analysis (synthesis and crystallography)
Assoc. Prof. Lukasz Kedzierski
Supervisor (Microbiology)
- Project Administration
- Funding Aquisition
Prof. Philip C. Andrews
Supervisor (Chemistry)
- Project Administration
- Funding Aquisition

Declaration of Competing Interest

There are no conflicts to declare.

Acknowledgements

The authors would like to thank the Australian Research Council (DP170103624) and Monash University for financial support. We would also like to thank Dr. Craig Forsyth (Monash) for assistance with X-ray crystallography. The authors would also like to acknowledge the Australian Synchrotron for use of the MX1 beamline at the Australian Synchrotron, part of ANSTO.

Appendix A. Supplementary data

Supplementary data to this article can be found online at https://doi.org/10.1016/j.jinorgbio.2021.111385.

References

[1] W.H. Organization, Weekly Epidemiological Record (WER) vol. 91, World Health Organization, 2016, pp. 285–296.
[2] W.H. Organization, Investing to Overcome the Global Impact of Neglected Tropical Diseases: Third WHO Report on Neglected Tropical Diseases. https://www.who.int/neglected_diseases/9789241564861/en/, 2015 (accessed Novermber 2020).
[3] J. Alvar, I.D. Vélez, C. Bern, M. Herrero, P. Desjeux, J. Cano, J. Jannin, M. den Boer, W.L.C. Team, PLoS One 7 (2012) e35671.
[4] W.H. Organization, Control of the Leishmaniases: Report of a WHO Expert Committee. https://apps.who.int/iris/bitstream/handle/10665/227957/WER6612_88-88.PDF, 1990 (accessed November 2020).
[5] A. Stauch, H.-P. Duerr, J.-C. Dujardin, M. Vanaerschot, S. Sundar, M. Eichner, PLoS Negl. Trop. Dis. 6 (2012), e1973.
[6] J. van Griensven, M. Balasegaram, F. Meheus, J. Alvar, L. Lynen, M. Boelaert, Lancet Infect. Dis. 10 (2010) 184–194.
[7] H. Sun, Biological Chemistry of Arsenic, Antimony and Bismuth, Wiley Online Library, 2011.
[8] M. Ouellette, J. Drummelsmith, B. Papadopoulou, Drug Resist. Updat. 7 (2004) 257–266.
[9] S.L. Croft, J. Engel, Trans. R. Soc. Trop. Med. Hyg. 100 (2006) S4–S8.
[10] S. Sundar, T.K. Jha, C.P. Thakur, S.K. Bhattacharya, M. Rai, Trans. R. Soc. Trop. Med. Hyg. 100 (Supplement 1) (2006) S26–S33.
[11] S. Sundar, K. Kumar, J. Chakravarty, D. Agrawal, S. Agrawal, A. Chhabra, V. Singh, Trans. R. Soc. Trop. Med. Hyg. 100 (2006) 698–700.
[12] L.H. Freitas-Junior, E. Chatelain, H.A. Kim, J.L. Siqueira-Neto, Int. J. Parasitol. Drugs Drug Resist. 2 (2012) 11–19.
[13] P. Shaked-Mishan, N. Ulrich, M. Ephros, D. Zilberstein, J. Biol. Chem. 276 (2001) 3971–3976.
[14] C. dos Santos Ferreira, P.S. Martins, C. Demicheli, C. Brochu, M. Ouellette, F. Frézard, Biometals 16 (2003) 441–446.

[15] R. Mukhopadhyay, S. Dey, N. Xu, D. Gage, J. Lightbody, M. Ouellette, B.P. Rosen, Proc. Natl. Acad. Sci. 93 (1996) 10383–10387.
[16] J.D. Berman, Clin. Infect. Dis. 10 (1988) 560–586.
[17] J.H. No, Acta Trop. 155 (2016) 113–123.
[18] A. Ponte-Sucre, F. Gamarro, J.-C. Dujardin, M.P. Barrett, R. López-Vélez, R. García-Hernández, A.W. Pountain, R. Mwenechanya, B. Papadopoulou, PLoS Negl. Trop. Dis. 11 (2017), e0006052.
[19] P.L. Olliaro, Curr. Opin. Infect. Dis. 23 (2010) 595–602.
[20] P.J. Hotez, N.C. Lo, in: E.T. Ryan, D.R. Hill, T. Solomon, N.E. Aronson, T.P. Endy (Eds.), Hunter's Tropical Medicine and Emerging Infectious Diseases, 10th edition, 2020, pp. 209–213 (London).
[21] H. Husein-ElAhmed, U. Gieler, M. Steinhoff, J. Eur. Acad. Dermatol. Venereol. 34 (10) (2020) 2216–2228.
[22] P. Wei, Z. Ye, S. Cao, S. Bai, P.H. Seeberger, J. Yin, J. Hu, Colloids Surf. A Physicochem. Eng. Asp. (2020) 124804.
[23] H. Ahmed, C.R. Curtis, S. Tur-Gracia, T.O. Olatunji, K.C. Carter, R.A. Williams, RSC Med. Chem. 11 (2020) 905–912.
[24] M.A.F. Gomes, L.L.C.d. Medeiros, F.P.D. Lobo, N.R.S. Wanderley, A.P.R. Matos, T. d.N. Jácome, M.G.L. Monteiro, K.G. Luz, Rev. Soc. Bras. Med. Trop. 51 (2018) 393–396.
[25] M.I. Ali, M.K. Rauf, A. Badshah, I. Kumar, C.M. Forsyth, P.C. Junk, L. Kedzierski, P. C. Andrews, Dalton Trans. 42 (2013) 16733–16741.
[26] R.N. Duffin, V.L. Blair, L. Kedzierski, P.C. Andrews, Dalton Trans. 47 (2018) 971–980.
[27] R.N. Duffin, V.L. Blair, L. Kedzierski, P.C. Andrews, J. Inorg. Biochem. 189 (2018) 151–162.
[28] T. Iftikhar, M.K. Rauf, S. Sarwar, A. Badshah, D. Waseem, M.N. Tahir, A. Khan, K. M. Khan, G.M. Khan, J. Organomet. Chem. 851 (2017) 89–96.
[29] A. Islam, J.G. Da Silva, F.M. Berbet, S.M. da Silva, B.L. Rodrigues, H. Beraldo, M. N. Melo, F. Frézard, C. Demicheli, Molecules 19 (2014) 6009–6030.
[30] Y.C. Ong, V.L. Blair, L. Kedzierski, P.C. Andrews, Dalton Trans. 43 (2014) 12904–12916.
[31] Y.C. Ong, V.L. Blair, L. Kedzierski, K.L. Tuck, P.C. Andrews, Dalton Trans. 44 (2015) 18215–18226.
[32] S. Sarwar, T. Iftikhar, M.K. Rauf, A. Badshah, D. Waseem, M.N. Tahir, K.M. Khan, G.M. Khan, Inorg. Chim. Acta 476 (2018) 12–19.
[33] R.N. Duffin, V.L. Blair, L. Kedzierski, P.C. Andrews, J. Inorg. Biochem. 203 (2020) 110932.
[34] J. Hodgson, Nat. Biotechnol. 19 (2001) 722–726.
[35] A.K. Renfrew, Metallomics 6 (2014) 1324–1335.
[36] A. Albert, M. Gibson, S. Rubbo, Br. J. Exp. Pathol. 34 (1953) 119.
[37] A. Albert, S. Rubbo, R. Goldacre, B. Balfour, Br. J. Exp. Pathol. 28 (1947) 69.
[38] J.H. Jeon, C.-H. Lee, H.-S. Lee, J. Korean Soc. Appl. Biol. Chem. 52 (2009) 202–205.
[39] A.R. Timerbaev, Metallomics 1 (2009) 193–198.
[40] É.A. Enyedy, O. Dömötör, K. Bali, A. Hetényi, T. Tuccinardi, B.K. Keppler, J. Biol. Inorg. Chem. 20 (2015) 77–88.
[41] M.C. Duarte, L.M. dos Reis Lage, D.P. Lage, J.T. Mesquita, B.C.S. Salles, S. N. Lavorato, D. Menezes-Souza, B.M. Roatt, R.J. Alves, C.A.P. Tavares, Vet. Parasitol. 217 (2016) 81–88.
[42] T. Agner, T. Menné, Contact Dermatitis 29 (1993) 163.
[43] P. Hongmanee, K. Rukseree, B. Buabut, B. Somsri, P. Palittapongarnpim, Antimicrob. Agents Chemother. 51 (2007) 1105–1106.
[44] H.M. Robinson Jr., M.B. Hollander, J. Invest. Dermat. 26 (1956) 143–147.
[45] A.K. Fisher, F.G. Walter, S. Szabo, J. Toxicol. Clin. Toxicol. 31 (1993) 113–120.
[46] R. Swain, J. Bapna, A. Das, S. Chandrasekar, R. Swaminathan, B. Bosco, S. Veliath, D. Thombre, Hum. Toxicol. 5 (1986) 35–41.
[47] H. Nahrevanian, M. Farahmand, Z. Aghighi, M. Assmar, A. Amirkhani, Pharmacological evaluation of antileishmanial activity by in vivo nitric oxide modulation in BALB/c mice infected with Leishmania major MRHO/IR/75/ER: an Iranian strain of cutaneous leishmaniasis, Exp. Parasitol. 116 (2007) 233–240.
[48] J. Mookerjee Basu, A. Mookerjee, P. Sen, S. Bhaumik, P. Sen, S. Banerjee, K. Naskar, S.K. Choudhuri, B. Saha, S. Raha, S. Roy, Antimicrob. Agents Chemother. 50 (2006) 1788–1797.
[49] A. Pathak, V.L. Blair, R.L. Ferrero, L. Kedzierski, P.C. Andrews, J. Inorg. Biochem. 1 (77) (2017) 266–275.
[50] O. Shimony, C.L. Jaffe, J. Microbiol. Methods 75 (2008) 196–200.
[51] J. Mikus, D. Steverding, Parasitol. Int. 48 (2000) 265–269.
[52] K. Lackovic, J.P. Parisot, N. Sleebs, J.B. Baell, L. Debien, K.G. Watson, J.M. Curtis, E. Handman, I.P. Street, L. Kedzierski, Antimicrob. Agents Chemother. 54 (2010) 1712–1719.
[53] K. Hensley, S. Mou, Q.N. Pye, Met. Biol. Oxidat. Stress. (2003) 185–193 (Springer).
[54] A. Wojtala, M. Bonora, D. Malinska, P. Pinton, J. Duszynski, M.R. Wieckowski, Methods Enzymol. 542 (2014) 243–262 (Elsevier).
[55] CrysAlisPro, CrysAlisPro version 1.171.40.49a, Rigaku Oxford Diffraction Ltd, Oxfordshire England, 2015 [56] B. AXS, Madison, vol. US, 2014.
[56] Bruker-Nonius, Apex-II. SAINT-plus (version 7.06a), Bruker AXS Inc, Wisconsin USA, 2004.
[57] George M. Sheldrick, A short history of SHELX, Acta Crystallographica Section A: Foundations of Crystallography 64 (1) (2008) 112–122.
[58] O.V. Dolomanov, L.J. Bourhis, R.J. Gildea, J.A. Howard, H. Puschmann, J. Appl. Crystallogr. 42 (2009) 339–341.
[59] T.M. McPhillips, S.E. McPhillips, H.-J. Chiu, A.E. Cohen, A.M. Deacon, P.J. Ellis, E. Garman, A. Gonzalez, N.K. Sauter, R.P. Phizackerley, J. Synchrotron Radiat. 9 (2002) 401–406.
[60] W. Kabsch, J. Appl. Crystallogr. 26 (1993) 795–800.
[61] D.V. Moiseev, Y.B. Malysheva, A.S. Shavyrin, Y.A. Kurskii, A.V. Gushchin, J. Organomet. Chem. 690 (2005) 3652–3663.
[62] H. Meinema, E. Rivarola, J. Noltes, J. Organomet. Chem. 17 (1969) 71–81.
[63] L. Saleem, A.A. Altaf, A. Badshah, M.K. Rauf, A. Waseem, M. Danish, S.S. Azam, M. N. Arshad, A.M. Asiri, S. Ahmad, Inorg. Chim. Acta 474 (2018) 148–155.
[64] V. Sharutin, O. Sharutina, E. Artem'eva, M. Makerova, Russ. J. Gen. Chem. 86 (2016) 2671–2676.
[65] M.N. Rocha, P.M. Nogueira, C. Demicheli, L.G. de Oliveira, M.M. da Silva, F. Frézard, M.N. Melo, R.P. Soares, Bioinorg. Chem. Appl. 2013 (2013).
[66] L.G.d. Oliveira, M.M. Silva, F. Paula, E.C. Pereira-Maia, C.L. Donnici, C.A. d. Simone, F. Frézard, E.N. Júnior, C. Demicheli, Molecules 16 (2011) 10314–10323.
[67] V.K. Cherkasov, G.A. Abakumov, E.V. Grunova, A.I. Poddel'sky, G.K. Fukin, E. V. Baranov, Y.V. Kurskii, L.G. Abakumova, Chem. Eur. J. 12 (2006) 3916–3927.
[68] H. Barucki, S.J. Coles, J.F. Costello, M.B. Hursthouse, J. Organomet. Chem. 622 (2001) 265–273.
[69] H. Barucki, S.J. Coles, J.F. Costello, T. Gelbrich, M.B. Hursthouse, Dalton Trans. (2000) 2319–2325.
[70] G.-C. Wang, Y.-N. Lu, J. Xiao, L. Yu, H.-B. Song, J.-S. Li, J.-R. Cui, R.-Q. Wang, F.-X. Ran, J. Organomet. Chem. 690 (2005) 151–156.
[71] B.F. Hoskins, E.R. Tiekink, G. Winter, Inorg. Chim. Acta 97 (1985) 217–222.
[72] A.K. Jami, V. Baskar, Dalton Trans. 41 (2012) 12524–12529.
[73] T. Westhoff, F. Huber, R. Rüther, H. Preut, J. Organomet. Chem. 352 (1988) 107–113.
[74] T. Westhoff, F. Huber, H. Preut, J. Organomet. Chem. 348 (1988) 185–191.
[75] N.C. Norman, Chemistry of Arsenic, Antimony and Bismuth, Blackie Academic and Professional, 1997.
[76] A. Nimmermark, L. Öhrström, J. Reedijk, Z. Krist-Cryst. Mater. 228 (2013) 311–317.
[77] R.D. Abughazaleh, T.S. Tracy, Wiley Encyclopedia of Clinical Trials, 2007.
[78] E. Handman, in: J.R. Baker, R. Muller, D. Rollinson (Eds.), Adv. Parasitol. vol. 44, Academic Press, 1999, pp. 1–39.
[79] M.F. Horta, B.P. Mendes, E.H. Roma, F.S.M. Noronha, J.P. Macêdo, L.S. Oliveira, M.M. Duarte, L.Q. Vieira, J. Parasit. Res. 2012 (2012).
[80] J.A. Imlay, EcoSal Plus vol. 3, 2009.
[81] T. Naderer, M.J. McConville, Cell. Microbiol. 10 (2008) 301–308.
[82] J. MacMicking, Q.-w. Xie, C. Nathan, Annu. Rev. Immunol. 15 (1997) 323–350.
[83] R. Olekhnovitch, P. Bousso, Trends Parasitol. 31 (2015) 653–664.
[84] R.N. Duffin, V.L. Blair, L. Kedzierski, P.C. Andrews, Eur. J. Med. Chem. (2019) 111895.
[85] C. Ferreira, D. Soares, C. Barreto-Junior, M. Nascimento, L. Freire-de-Lima, J. Delorenzi, M. Lima, G. Atella, E. Folly, T. Carvalho, Phytochemistry 72 (2011) 2155–2164.
[86] N.G. Tessarollo, J.M. Andrade, D.d.S. Moreira, S.M.F. Murta, Parasitol. Int. 64 (2015) 125–129.
[87] S. Rais, A. Perianin, M. Lenoir, A. Sadak, D. Rivollet, M. Paul, M. Deniau, Antimicrob. Agents Chemother. 44 (2000) 2406–2410.